



Cite this: *RSC Adv.*, 2015, 5, 49270

Tribochemistry of phosphorus additives: experiments and first-principles calculations†

M. I. De Barros-Bouchet,^{*a} M. C. Righi,^{*b} D. Philippon,^a S. Mambingo-Doumbe,^c T. Le-Mogne,^a J. M. Martin^a and A. Bouffet^c

Organophosphorus compounds are common additives included in liquid lubricants for many applications, in particular automotive applications. Typically, organic phosphites function as friction-modifiers whereas phosphates as anti-wear additives. While the antiwear action of phosphates is now well understood, the mechanism by which phosphites reduce friction is still not clear. Here we study the tribochemistry of both phosphites and phosphates using gas phase lubrication (GPL) and elucidate the microscopic mechanisms that lead to the better frictional properties of phosphites. In particular, by *in situ* spectroscopic analysis we show that the friction reduction is connected to the presence of iron phosphide, which is formed by tribochemical reactions involving phosphites. The functionality of elemental phosphorus in reducing the friction of iron-based interfaces is elucidated by first principle calculations. In particular, we show that the work of separation and shear strength of iron dramatically decrease by increasing the phosphorus concentration at the interface. These results suggest that the functionality of phosphites as friction modifiers may be related to the amount of elemental phosphorus that they can release at the tribological interface.

Received 13th January 2015
Accepted 21st May 2015

DOI: 10.1039/c5ra00721f

www.rsc.org/advances

1. Introduction

Organophosphorus compounds are important extreme pressure (EP) and anti-wear (AW) additives used in different industrial fields, especially automotive applications.^{1,2} While phosphate ester additives were extensively investigated during the last few decades,^{3–9} few studies have been devoted to phosphite compounds despite their increasing use in engine oils,^{10–16} especially for gearbox components. Among the wide variety of phosphite additives used to improve the oil friction reduction performances, the most common ones are triallyl-phosphite, tributyl-phosphite, dilauryl-phosphite, dioleil-phosphite and triphenyl-phosphite. The chemical structure of these additives greatly influences the nature of the formed tribofilm and its tribological performances. Riga *et al.*¹⁶ showed that shorter phosphite chains give better anti-wear performances. This seems to be related to the formation of a tribofilm containing iron phosphide that was identified by Barcroft¹⁷ as Fe₂P on rubbed surfaces lubricated by tricresyl-phosphate (TCP). The lubrication mechanism of TCP was attributed to a polishing action *via* the formation of an iron/iron phosphide eutectic.¹⁸ In

a previous publication,¹⁹ Philippon *et al.* evidenced clearly the formation of iron phosphide species from trimethyl-phosphite (TMPi) molecules and they detailed the reaction mechanism of TMPi on an iron surface. They also investigated the role of the freshly nascent surfaces obtained by friction in UHV on the decomposition of the TMPi molecules using gas phase lubrication (GPL) approach thanks to an environmentally controlled analytical tribometer (ECAT).²⁰ The *in situ* chemical analysis clearly gave some evidence of the chemical dissociation of TMPi on iron surfaces under friction leading to the formation of iron phosphide compound which was fully characterized by focused ion beam/high resolution transmission microscopy (FIB/HRTEM).²¹

GPL is not a new concept in lubrication technology, but it is a well-known way to lubricate systems subject to high temperatures, as those present in cutting and working metal processes for example.^{22,23} It has been shown that GPL is able to simulate the boundary lubrication regime by bringing directly the molecules on the surface in contact,^{24,25} thus avoiding the use of solvents for cleaning the rubbed surfaces prior to spectroscopic analyses and therefore reducing the risk of their contamination and/or denaturation. This is a huge advantage compared to standard liquid phase lubrication coupled with *ex situ* post mortem surface analyses. Using this approach, the effect of active nascent metallic surfaces on decomposition of adsorbed molecules was highlighted^{20,26,27} and the importance of dangling bonds passivation to achieve low friction in carbon-based materials was evidenced.^{28,29}

Here, we performed GPL experiments coupled with *in situ* surface analyses to investigate the tribochemistry of different

^aLaboratoire de Tribologie et Dynamique des Systèmes, Ecole Centrale de Lyon, Université de Lyon, 69134 Ecully, France. E-mail: maria-isabel.de-barros@ec-lyon.fr

^bCNR Istituto di Nanoscienze Centro S3, Dipartimento di Fisica, Università di Modena e Reggio Emilia, 41100 Modena, Italy. E-mail: mcRighi@unimore.it

^cTOTAL, Centre de Recherche de Solaize, 69360 Solaize, France

† Electronic supplementary information (ESI) available. See DOI: 10.1039/c5ra00721f

phosphorus-containing organic additives. We consider trimethyl phosphate (TMPa), trimethyl phosphite (TMPi) and dimethyl phosphite (DMPi), respectively. The latter exists in two different chemical equilibrium states, namely the phosphite and the phosphonate. These molecules present the same chemical groups as commercial organo-phosphorus additives, but have shorter hydrocarbon chains. This allowed us to use them in the gas phase, without losing any information on tribological effects. The main functionality of the hydrocarbons groups is, in fact, to solubilize or micellize the additive molecules into the base oil. We found that phosphites reduce friction more efficiently than phosphates and their friction reduction property is directly related to the tribo-induced formation of iron phosphide. The measured friction coefficient decreases, in fact, as the amount of iron phosphide observed after the tribological experiment increases, TMPi presenting the lowest friction coefficient.

To shed light into these experimental observations, we performed first principles calculations of the interfacial properties of adhesion and shear strength. The knowledge of these intrinsic properties of materials in contact is important to interpret their tribological behavior, in particular to provide a microscopic understanding on the functionality of lubricant additives. In boundary lubrication conditions, where hydrodynamic lubrication is no longer effective, the friction reduction and wear protection is provided by the tribofilm formed by the chemical additives reaction on the sliding surfaces. Indeed, these compounds react with the surfaces and modify their chemical composition, with consequent modifications of their adhesion and resistance to sliding. First-principle calculations based on density functional theory are able to provide an accurate description of the surface chemistry and its effects on the surface–surface interactions, such accuracy is typically unattainable by classical force fields based on empirical parameterizations of the atomic interactions. However, the use of first-principle calculations in tribochemistry has been traditionally very scarce, despite their widespread use in surface and interface science. Here, we show that first-principle calculations can be successfully applied to study the effects of lubricant additives. In particular, we show that elemental phosphorus, released at the interface as product of tribochemical reactions involving phosphites, can highly reduce the adhesion between two iron surfaces. Moreover, the frictional forces that develop during sliding are much lower in the presence of interfacial phosphorus than oxygen at the same concentration. These results offer a possible explanation for the observed different tribological behavior of TMPi and TMPa and suggest an important, new conclusion for understanding the functionality of organophosphorus additives: a key feature to reduce friction might be related to the ability of the compound to release elemental phosphorus at the tribological interface.

II. Methodology

Device and methods for GPL

ECAT is a specific apparatus home-built at Ecole Centrale de Lyon (ECL) and dedicated to GPL. It is composed of two independent parts: a UHV chamber dedicated to friction experiments

under an environmentally controlled gas phase (named Environmentally Controlled Tribometer, ECT) and a second UHV chamber dedicated to surface analyses (XPS and Auger spectroscopies). The ECAT is schematically presented in Fig. 1. A reciprocating pin-on-flat machine with a movable hemispherical pin being connected to a brushless motor is located inside ECT. The temperature of the friction contact can be controlled from $-100\text{ }^{\circ}\text{C}$ to $600\text{ }^{\circ}\text{C}$ thanks to the flat holder equipped with a nitrogen cooling and a heating system. Both normal and tangential forces are accurately measured thanks to optical sensors. The ECT is able to measure both super-low friction (milli-range) and very high (above unity) friction coefficients. A pure gas or a gas mixture can be introduced inside the ECT by using 3 micro-leak valves and their pressure can be continuously varied from 10^{-9} hPa to 2000 hPa (twice the atmospheric pressure), thanks to a membrane vacuum gauge. The tribometer is computer-controlled and the normal load is automatically adjusted when the gas pressure inside the ECT is changed. The pin-on-flat contact can be optically observed sideways by a low level SIT camera. The ECT is connected to the analysis chamber by a third intermediate UHV chamber allowing the transfer of the rubbed surfaces without any exposure to air.

Heavy molecular weight compounds like triphenyl-phosphite and tricresyl-phosphate are used as additives in commercial lubricants because of the solubility in oil provided by the presence of long carbon chains in the molecule. However, it is difficult to evaporate these heavy molecular weight additives in a vacuum. Therefore smaller molecules, having the same chemical function, were used as phosphite/phosphate model molecules for GPL, namely TMPi, DMPi and TMPa having a purity of 99+% (>99%), provided by the Aldrich Chemical Co. These molecules were further purified by freeze pumping thaw cycles before being introduced into the ECT. Table 1 provides the chemical formula, molecular weights and the saturating vapor pressures (SVP) at room temperature for these three compounds. The DMPi compound is interesting because it presents two chemical equilibrium states, the first one is the phosphite form in which the P atom is trivalent and the second one is the phosphonate form in which the P atom is pentavalent. GPL experiments in the presence of these compounds were carried out with AISI 52100 steel friction pairs (96.9Fe–1.04C–1.45Cr–0.35Mn–0.27Si (wt%)). All samples were polished with a diamond solution and cleaned with *n*-heptane and 2-propanol ultrasonic baths, afterwards. The surface roughness obtained is varying between 20–25 nm in Ra. The hemispherical pin has a curvature radius of 8 mm. The both friction specimens, pin and flat, are brought into contact once the gas pressure reaches the required value inside the ECT (see Fig. 1) with a normal load of 3.5 N corresponding to a maximum Hertzian contact pressure of 0.52 GPa. The linear reciprocating motion was running during GPL experiments at ambient temperature ($25\text{ }^{\circ}\text{C}$) with a sliding speed of 0.5 mm s^{-1} and a track length of about 2 mm.

Systems and methods of first principles calculations

We performed spin-polarized density functional theory calculations, using the Perdew–Burke–Ernzerhof (PBE) generalized gradient approximation for the exchange correlation

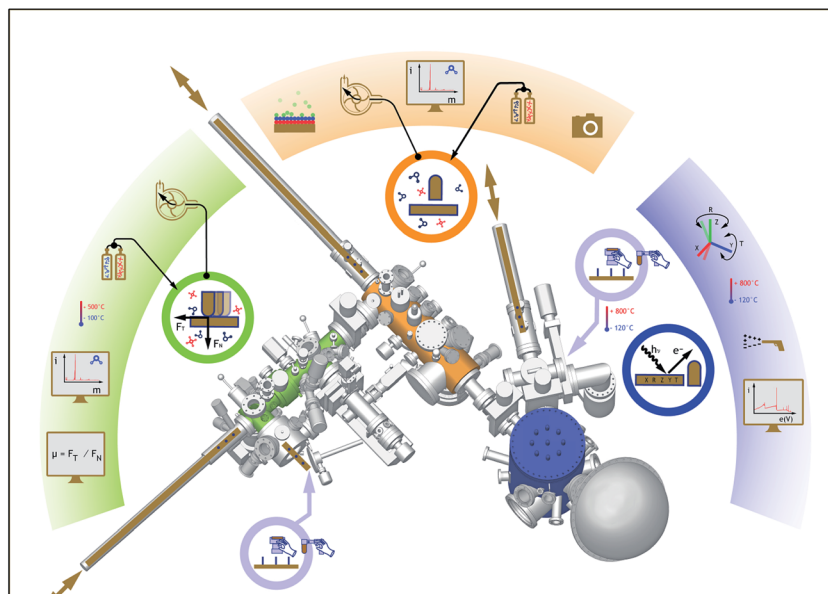


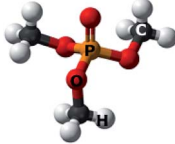
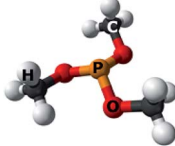
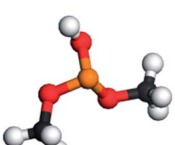
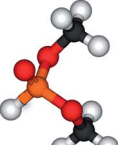
Fig. 1 Schematic view of the Environmentally Controlled Analytical Tribometer (ECAT) developed at ECL. The green part is the ECT, the orange part is an intermediate preparation chamber and the blue one is the XPS/AES analysis chamber.

functional.³⁰ The electronic wave-functions were expanded in plane waves and the ionic species were described by ultrasoft-pseudopotentials. Semi-core states (3s, 3p) of iron were considered as valence states. On the basis of test calculations, we used 30 Ry (240 Ry) cutoff for truncating the wave-function (charge density) expansion.

We considered the Fe(110) surface since it is the most stable among densely packed iron surfaces.³¹ It is known that this

surface does not reconstruct, but presents relaxation. The surface was modeled by means of periodic supercells containing an iron slab and a vacuum region 20 Å thick. We considered three-layer thick slabs, which we tested against thicker slabs to represent a good compromise between calculation accuracy and computational efficiency. In particular, we studied P adsorption at the Fe(110) surface both by using three-layer and five-layer thick slabs and we found that the geometries obtained in the

Table 1 Chemical formula, molecular weight and SVP at room temperature of TMPi, TMPa, and DMPI

| Model molecule | Chemical formula | Molecular weight (g mol ⁻¹) | SVP at room temperature (hPa) |
|--|---|---|-------------------------------|
| Trimethyl-phosphate (TMPa) |  | 140 | 1.1 |
| Trimethyl-phosphite (TMPi) |  | 124 | 22.6 |
| Dimethyl-phosphite (DMPi) |  | 110 | 30 |
| Dimethyl-hydrogen dymethyl-phosphonate phosphite |  | | |

two cases are similar and the energy differences among different sites are preserved (they change by less than 4%). The supercell Brillouin zone was sampled by means of a Monkhorst–Pack grid equivalent to 8×8 in the surface unit cell.

The interfaces were modeled by means of supercells having a vertical edge 28 Å long and containing two slabs in contact. The first interfacial property that we considered is the work of separation, W_{sep} , defined as the energy per unit area required to separate two surfaces from contact to an ideally infinite separation. In other words, W_{sep} corresponds to the difference between the formation energy of two isolated surfaces and the formation energy of an interface: $W_{\text{sep}} = \gamma_1 + \gamma_2 - \gamma_{12}$. By definition of W_{sep} it is assumed that the separated slabs have the same composition of the two slabs joint together to form the interface, therefore the work of separation can be calculated as a difference between total energies: $W_{\text{sep}} = (E_1 + E_2 - E_{12})/A$, where A is the supercell in-plane size, E_{12} is the total energy of the supercell containing two slabs in contact and E_1 (E_2) is the total energy of the same supercell containing only the upper (lower) slab (both the two- and one-slab systems are considered in their optimized configuration, *i.e.*, a relaxation process is carried out). The thickness of the vacuum region present in the supercell adopted in our calculation (about 22 Å (16 Å) in the case of one-(two-)slab system) is enough to isolate the system from its periodic replicas.

We calculated E_{12} for different relative lateral positions of the two surfaces in contact. At each location the structural relaxation was carried out by keeping fixed the bottom layer of the lower slab and optimizing all the other degrees of freedom except for the (x, y) coordinates of the topmost layer of the upper slab. In this way, the distance between the two surfaces could reach its equilibrium value, z_{eq} , at each fixed lateral position. By exploiting the system symmetries and interpolating, we constructed the potential energy surface (PES), $E_{12}(x, y, z_{\text{eq}})$, which describes the variation of the interfacial energy as a function of surface relative lateral position. The absolute minimum of the PES is considered to calculate the work of separation of each interface.

The second interfacial quantity that we considered is the static friction force per unit area, τ . We calculated τ along selected symmetry directions from the derivatives of the PES profile along that directions.³²

III. Results and discussion

Tribochemistry of organophosphorus compounds

a. Friction results under GPL. For the GPL experiments, once the stabilization of the desired gas partial pressure in the ECT obtained, the friction experiment is started and the coefficient is measured for each reciprocating sliding cycles. The steady-state friction coefficient obtained after about 300 passes duration is reported as a function of TMPi and TMPa gas pressures in Fig. 2. Each experiment carried out at one desired pressure and corresponding to one specific track is repeated 3 times. Using the same flat and pin samples, several tests on different tracks are obtained by increasing progressively the gas pressure. This is made possible by translating the flat and

turning the extremity of the pin, and this between each successive test.

From Fig. 2, we can see that friction is reduced durably with respect to UHV ($\mu > 1$) when the gas pressure reaches the values of 10^{-2} hPa and 1 hPa for TMPi and TMPa, respectively. The reduction of the friction coefficient with the increase of gas pressure is a general trend that has been observed for many molecules.²⁵ This is generally explained by the need to have a critical dynamic covering rate of the surface by the molecules in order to lubricate the contact efficiently between two successive passes. From Fig. 2, a higher adsorption activity of TMPi on the iron surface is then demonstrated compared to TMPa. We can also observe that the steady-state friction value obtained for high gas pressure is close to that obtained in liquid phase lubrication with a traditional friction machine with similar tribological conditions.

Fig. 3 shows results obtained at longer friction experiments carried out with 1 hPa of TMPa and 1 hPa of TMPi. It appears that the phosphite reduces friction more efficiently than the phosphate for a gas pressure close to the saturating vapor pressure.

The friction coefficient obtained in the presence of 1 hPa of DMPi is also reported for comparison. The friction reaches a steady-state value of about 0.23 for TMPi, 0.34 for DMPi and 0.46 for TMPa. The values obtained for TMPi and TMPa are in good correlation with the steady-state friction coefficients obtained in liquid phase friction tests in the same conditions, *i.e.* 0.21 for TMPi and 0.37 for TMPa (see Fig. 2). The wear tracks formed on the surface of the steel flats at the end of the experiments in the presence of TMPi and TMPa were observed by optical microscopy (Fig. 4). A tribofilm was clearly evidenced for TMPi and a lot of debris is present around the track, especially at the extremities. For TMPa, the tribofilm was more difficult to observe because it seems optically transparent. However, the three gases seem to have similar good anti-wear properties because the width of the wear tracks on the steel flats and the diameter of the wear tracks on the hemispherical pins (not shown here) almost correspond to the calculated initial Hertzian diameter, *i.e.* 114 μm . Indeed, the functionality of phosphites as friction modifiers appears to be the main difference in comparison with the phosphates-based additives. The different frictional behaviors of these phosphorus-based compounds can be related to the chemical nature of the formed tribofilms.

To check this assumption, *in situ* surface analyses were carried out inside and outside the wear tracks formed on the flats immediately after the friction experiments. This is made possible by transferring the steel flats from ECT to the analysis chamber thanks to the UHV intermediate preparation chamber (see Fig. 1).

b. Friction reduction mechanism studied by *in situ* XPS analysis. Chemical speciations of phosphorus and iron atoms were accurately identified thanks to XPS chemical shifts. Fortunately, ion etching that is usually used to remove carbon contamination in *post-mortem* analyses was not necessary here because the samples are never in contact with air in the ECAT. *In situ* XPS spectra for elements of interest (C1s, O1s, Fe2p^{3/2})

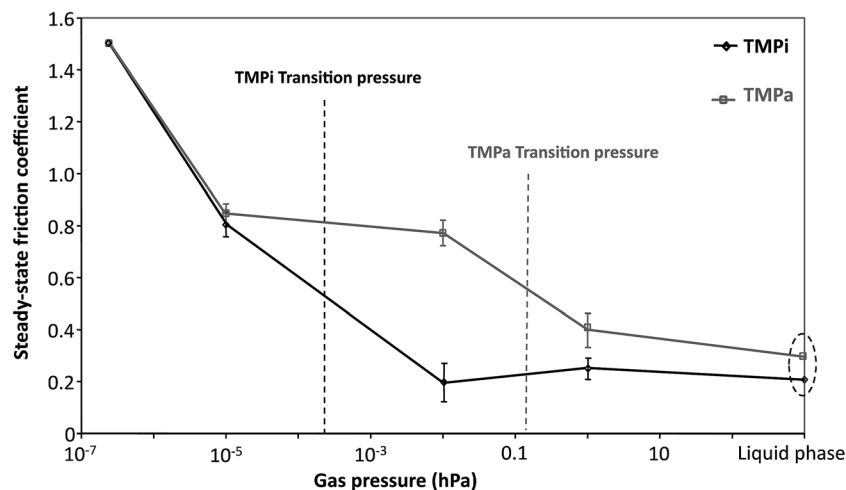


Fig. 2 Steady-state friction coefficient obtained under GPL at room temperature for steel/steel friction pair at various gas pressures of TMPI and TMPa.

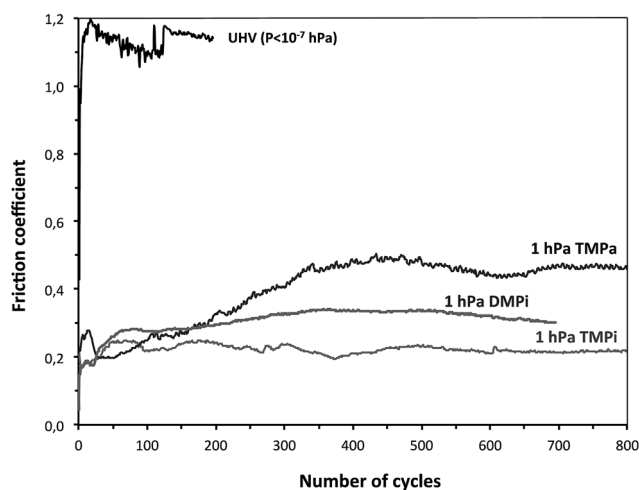


Fig. 3 Evolution of the friction coefficients obtained for steel/steel friction pair under GPL in the presence of 1 hPa of TMPI, 1 hPa of TMPa and 1 hPa of DMPi versus number of cycles at room temperature.

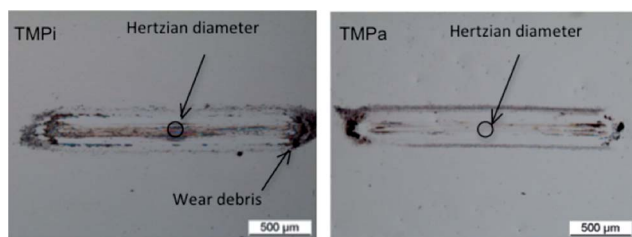


Fig. 4 Optical images of the wear tracks formed on the steel flats after the GPL experiments in the presence of 1 hPa of TMPI and 1 hPa of TMPa (see Fig. 3). The calculated Hertzian diameter is reported on each image for comparison.

and P2p) were recorded inside and outside the tribofilms formed with TMPI, DMPi and TMPa, respectively. Special attention was paid to the Fe2p^{3/2} and P2p spectra that provide

essential information about the chemical nature of the tribofilm. An interesting feature was observed on the P2p photopeak as shown in Fig. 5a: a new component at about 129 eV, which is present only after friction in the presence of TMPI and DMPi, but not with TMPa. It is attributed to phosphide chemical species according to XPS database.³³ Moreover, it is stronger in the case of TMPI than with DMPi, as shown by the XPS quantifications presented in Table 2. This is consistent with the dual chemical state of DMPi as discussed in the previous section. The second XPS peak observed inside the tribofilm has a higher binding energy of 133.6 eV for TMPI and 134.1 eV for TMPa. It is attributed to the adsorption of the inlet gaseous molecules on the surface of the tribofilm at the end of the friction experiment. Regarding the Fe2p^{3/2} spectra in Fig. 5b, for TMPI and DMPi, the contribution at about 707 eV is very intense compared to iron oxide at 710.5 eV. Moreover, it is also really intense compared to the same contribution for TMPa-derived tribofilm. This can be explained by the presence of an iron phosphide compound that is commonly found at a similar energy, *i.e.* about 707.1 eV for TMPI and DMPi. However, it is really difficult to distinguish the metallic iron Fe2p^{3/2} peak at about 707 eV from an iron phosphide one, which is at about 707.1 eV. Nonetheless, the good correlation between the Fe–P and P–Fe bonds quantifications for TMPI and DMPi and the small amount of this contribution for TMPa-derived tribofilm seems to confirm that it is iron phosphide. The significant advantage of *in situ* analyses here is that the different signals are not likely to change and/or masked by an oxidization in air as in the case of *ex situ* surface analyses performed after friction experiments in liquid phase. This explained why the iron phosphide contribution is clearly detected for TMPI and iron oxide contribution is particularly reduced. Therefore, iron phosphide is mainly generated during friction.

The different tribological behaviors of TMPa and TMPI can be explained thanks to the chemical hardness theory described by Pearson.³⁴ Indeed, the hard and soft acid base (HSAB) principle (or chemical hardness concept) can be used to predict the

preferential reactions between various chemical species. This principle was previously applied to tribological processes in boundary lubrication.³⁵ This principle specifies that a hard base prefers to react with a hard acid to form ionic compounds whereas a soft base prefers to react with a soft acid to form more covalent species. Table 3 summarizes the different possible species encountered in this study and their classification following the chemical hardness model. According to the HSAB principle, the TMPa molecule (hard base) preferentially reacts with iron oxide (strong acid) whereas the TMPi and DMPi, in its phosphite chemical state, (soft bases) preferentially react with metallic iron (soft acid). Therefore, according to the prediction of chemical hardness, TMPa prefers to react with the iron oxide present in the contact rather than with nascent metallic iron that may appear during wear.

To briefly summarize, our experimental data show that iron phosphide decreases more efficiently friction coefficient than iron phosphate. This result is corroborated by the behavior of the DMPi molecule having a dual character.

Effect of interfacial phosphorus on the adhesion and shear strength of iron interfaces by first principles calculations

The combined GPL experiment and spectroscopic analysis described above revealed that the ability of the considered organophosphorus additives to reduce friction increases with the amount of iron phosphide formed during the tribological

experiment. To shed light into this finding we performed a twofold analysis with the aim at elucidating (i) the microscopic mechanisms that lead to iron-phosphide formation through phosphite decomposition, (ii) the functionality of phosphorus in reducing friction of iron. Here we focus on second issue: we perform first principles calculations of the adhesion and shear strength of iron interfaces containing phosphorus in different concentrations and compare them to those of clean and oxygen-terminated interfaces.

It is well known that phosphorus segregates in iron and forms 2D chemisorbed overlayers,³⁶ but to our knowledge there is presently no information on their structure in the literature. We, then, identified the most favorable adsorption site for P at the Fe(110) surface by comparing the adatom energy at the high symmetry locations represented in Fig. 6a, namely on top (OT), short bridge (SB) and long bridge (LB). We found that the LB site, having the highest coordination, is the most stable adsorption location. The same result holds true for oxygen, in agreement with previous calculations.^{37,38} We, then, evaluated the effects of a coverage increase with respect to 0.25 ML (corresponding to one atom per 2×2 cell), and found that it destabilizes the overlayers. In particular, the adsorption energy per atom increases by 6% for a coverage increase to 0.5 ML (realized by a $c(2 \times 2)$ periodicity) and by 21% at full coverage.

The interfaces were modeled by self-mating the optimized surfaces represented in Fig. 6 and the adhesion energy was

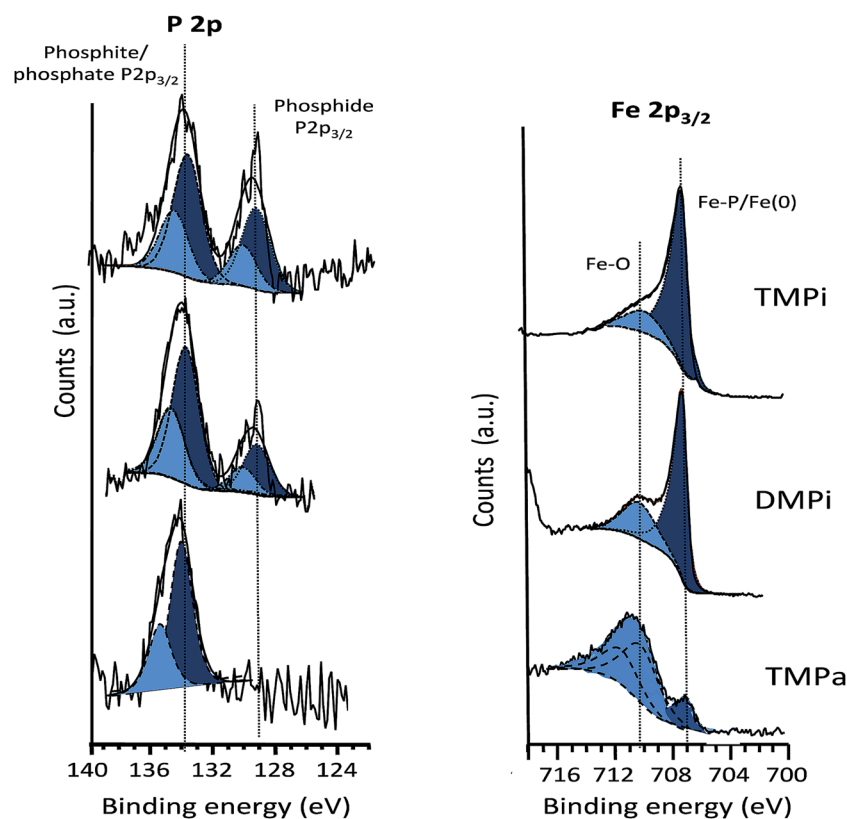


Fig. 5 High resolution XPS spectra recorded *in situ* on the tribofilms formed in the presence of TMPi, DMPi and TMPa at room temperature: (a) P2p core level and (b) Fe2p_{3/2} core level.

Table 2 Determination of the chemical species and atomic quantifications by *in situ* XPS analyses

| Compound | | Element | Bond | Energy (eV) | Concentration (% at.) |
|----------|-------------------|---------|-------|-------------|-----------------------|
| TMPi | Inside tribofilm | P | P-Fe | 129.1 | 7% |
| | | | P-O | 133.6 | 14% |
| | | Fe | Fe-P | 707.1 | 7% |
| | Outside tribofilm | P | Fe-O | 710.1 | 4% |
| | | | P-Fe | 129.1 | 0% |
| | | Fe | P-O | 133.6 | 10% |
| DMPi | Inside tribofilm | P | Fe-Fe | 707 | 5.2% |
| | | | Fe-O | 710.1 | 7.6% |
| | | Fe | P-Fe | 129.1 | 5.2% |
| | Outside tribofilm | P | P-O | 133.6 | 13.8% |
| | | | Fe-O | 710.1 | 6.5% |
| | | Fe | P-Fe | 129.1 | 0% |
| TMPa | Inside tribofilm | P | P-O | 133.6 | 5.1% |
| | | | Fe-Fe | 707 | 3.2% |
| | | Fe | Fe-O | 710.1 | 8.5% |
| | | P | P-Fe | 129 | 0% |
| | | | P-O | 134.1 | 2.5% |
| | | Fe | Fe-Fe | 707 | 0.7% |
| | | | Fe-O | 710.1 | 4.9% |

Table 3 Classification on the basis of the HSAB principle of different species according to Pearson³⁴ (the ones concerned by this study are in bold)

| | Acid | Base |
|------------|---|--|
| Hard | H ⁺ , Fe³⁺ , R ₃ C ⁺ | H ₂ O, OH ⁻ , O ²⁻ , PO₄³⁻ |
| Borderline | Fe ²⁺ , Cu ²⁺ | BO ₃ ³⁻ , N ₂ |
| Soft | Fe⁰ , Cu ⁺ , metal atoms | I ⁻ , CO, R ₂ S, (RO)₃P |

calculated for different relative lateral positions, constructing in this way the PES for the sliding interface. In Fig. 6 we compare the PESes of the bare interface and that obtained including interstitial phosphorus at an interfacial coverage of 0.25. A common energy scale is used, the blue color indicates the PES minimum, which is taken as reference and the red color is for the PES maximum. It appears evident that the effect of interfacial P is to consistently reduce the potential corrugation and hence the frictional forces.

A ball-stick representation of the optimized interface structures obtained for the PES minima is presented in Fig. 7, the corresponding work of separation, W_{sep} , and the distance between interfacial Fe layers, z_{eq} , are reported in Table 4. The shear strength, τ , calculated along the minimum energy paths (MEPs) identified for the [-110] and [001] sliding directions, from now on referred to as x and y directions, are also reported in Table 4. The procedure adopted to derive τ_x and τ_y is reported as ESI† as well as the PESes calculated for all the considered interfaces.

As can be seen in Fig. 6a, the minima of the PES for the clean interface are located at LB positions, *i.e.*, where a new layer would be positioned in the bcc structure of iron bulk. Two clean

iron surfaces in contact undergo a cold sealing (Fig. 7a): the optimized interfacial separation corresponds to the interlayer distance in Fe bulk, the work of separation W_{sep} is equal to the energy required to form two Fe(110) surfaces and the shear strength $\tau_{x,y} \sim 10$ GPa is typical of bulk iron.

The situation is completely altered if the mating surfaces are P-terminated. At interfacial coverage $\theta_p = 0.25$ (Fig. 7b) the distance between the interfacial Fe layers increases by 60% and the adhesion decreases by one order of magnitude with respect to the clean iron interface. A decreased adhesion gives rise to a smoother PES, as can be seen in Fig. 6b, and lower frictional forces: the shear stress decreases by 60%. Such consistent decrease of the shear strength is not observed in the case of O termination at the same coverage (Fig. 7e). A possible cause of this result resides in fact that O adsorbs more closely to the iron surface than P ($z_{\text{O}} - z_{\text{Fe}} = 1.01$ Å, $z_{\text{P}} - z_{\text{Fe}} = 1.48$ Å) and has a smaller atomic radius. Therefore, even if the amplitude of the potential modulation is similar in the two cases, its period is shorter in the case of oxygen, giving rise to a higher magnitude of forces, as illustrated in the ESI.†

In Fig. 7c and d it can be seen that by increasing the concentration of interfacial phosphorus to $\theta_p = 0.5$ and $\theta_p = 1$, the distance between the surfaces increases and chemical bonds are no longer present across the interface, the surfaces are held together by electrostatic and polarization interactions. The disappearance of chemical bonds produces a considerable decrease in the adhesion and shear strength³⁹ (last two rows of Table 4). In particular, in the case of two fully passivated surfaces in contact the short-range repulsion between interfacial P layers causes a decrease of adhesion and shear strength by two orders magnitude with respect to clean iron.

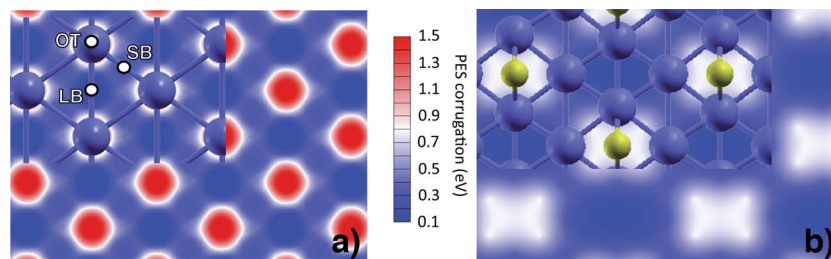


Fig. 6 Two-dimensional representation of the PESes obtained for the clean (a) and the P-containing iron interface (P atoms are in yellow) at relative concentration of 0.25 (b). A common energy scale is used for the potential corrugation.

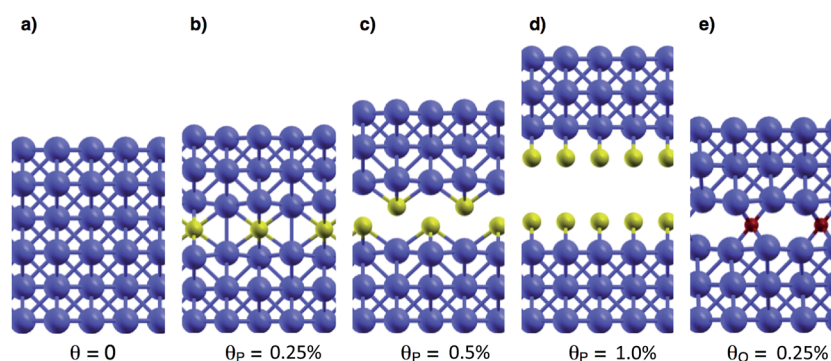


Fig. 7 Lateral view of the relaxed interface structures. The relative lateral position of the two mating surfaces corresponds to the absolute minimum of each PES.

Table 4 The work of separation, W_{sep} , and the equilibrium distance, z_{eq} , separating the innermost Fe layers at the interface are reported for the PES absolute minimum. The shear strengths, τ , are calculated for the MEPs along the $[-110]$ and $[001]$ sliding directions

| Interfacial coverage | W_{sep} | z_{eq} (Å) | τ_x (GPa) | τ_y (GPa) |
|----------------------|------------------|---------------------|----------------|----------------|
| $\theta = 0$ | 4.8 | 2.0 | 10.1 | 10.1 |
| $\theta_p = 0.25$ | 0.6 | 3.2 | 4.0 | 4.0 |
| $\theta_p = 0.5$ | 0.3 | 4.3 | 3.3 | 2.1 |
| $\theta_p = 1.0$ | 0.02 | 7.3 | 0.1 | 0.1 |
| $\theta_o = 0.25$ | 0.4 | 2.8 | 9.2 | 6.4 |

IV. Conclusions

We carried out experimental modeling of tribochemical reactions of different organophosphorus compounds by Gas Phase Lubrication. Selected gas molecules were used to simulate the chemical action of lubricant additives without providing any rheological contribution. Lubrication with TMPi and DMPi gases reduces friction more efficiently than the TMPa gas. This friction reduction is correlated with the formation iron phosphide in the tribofilm whereas TMPa-derived tribofilm is mainly composed of iron phosphate. DMPi molecules presenting two different chemical equilibrium states (phosphite and phosphonate) provide an intermediate friction behavior correlated with the formation of a

tribofilm containing less iron phosphide in comparison with TMPi-derived tribofilm.

The property of friction reduction related to iron phosphide formation is of particular interest because it points at the key role of elemental phosphorus in reducing the resistance to sliding of iron-base substrates. We confirmed this hypothesis by first principles calculations based on spin-polarized density functional theory. The adhesion and shear strength of phosphorus-containing iron interfaces were compared with those of clean and oxygen-terminated ones. The results clearly revealed that phosphorus is very efficient in reducing the resistance to sliding of iron on iron. The same is not observed for interfacial oxygen at the same concentration. Therefore, a possible explanation for the observed different tribological behavior of TMPi and TMPa can be proposed. On one hand phosphites produce higher amount of phosphorus than phosphates at the interface because the presence of oxygen has the drawback to limit the adsorption and dissociation of further incoming molecules. On the other hand, elemental phosphorus has been shown to dramatically reduce the resistance to sliding of native iron surfaces, which are exposed under tribological conditions.

Acknowledgements

The authors would like to thank the French ANR agency for financial support.

References

- 1 H. Spikes, The history and mechanisms of ZDDP, *Tribol. Lett.*, 2004, **17**(3), 469–489.
- 2 C. Minfray, J. M. Martin, M. I. De Barros Bouchet, T. Le Mogne and B. Hagenhoff, Chemistry of ZDDP tribofilm by ToF-SIMS, *Tribol. Lett.*, 2004, **17**(3), 351–357.
- 3 A. Gauthier, H. Montes and J. M. Georges, Boundary lubrication with tricresyl phosphate, *ASLE Trans.*, 1982, **25**(4), 445–455.
- 4 D. Godfrey, The lubrication mechanism of tricresyl-phosphate on steel, *ASLE Trans.*, 1965, **8**, 1–11.
- 5 M. N. Najman, M. Kasrai, G. M. Bancroft and A. Miller, Study of the chemistry of films generated from phosphate ester on 52100 steel using X-ray absorption spectroscopy, *Tribol. Lett.*, 2002, **13**(3), 209–218.
- 6 A. Rossi, F. M. Piras, D. Kim, A. J. Gellman and N. D. Spencer, Surface reactivity of tributyl thiophosphate: effects of temperature and mechanical stress, *Tribol. Lett.*, 2006, **23**, 197–208.
- 7 F. Gao, P. V. Kotvis, D. Stacchiola and W. T. Tysoe, Reaction of tributyl phosphate with oxidized iron: surface chemistry and tribology significance, *Tribol. Lett.*, 2005, **18**, 377–384.
- 8 D. Ren and A. J. Gellman, Reaction mechanism in organophosphate vapor phase lubrication of metal surfaces, *Tribol. Int.*, 2001, **34**, 353–365.
- 9 D. Sung and A. J. Gellman, Thermal decomposition of tricresyl phosphate isomers on Fe, *Tribol. Lett.*, 2002, **13**, 9–14.
- 10 W. Liu, L. Hu and Z. Zhang, Friction and wear of the film formed in the immersion test of oil containing antiwear and extreme pressure additives, *Thin Solid Films*, 1995, **271**, 88–91.
- 11 W. Liu and Q. Xue, Friction and wear of the film formed in an oil immersion test under nitrogen atmosphere, *Thin Solid Films*, 1997, **295**, 19.
- 12 D. Ren and A. J. Gellman, Initial steps in the surface chemistry of vapor phase lubrication by organophosphorus compounds, *Tribol. Lett.*, 1999, **6**, 191–194.
- 13 F. Gao, O. Furlong, P. V. Kotvis and W. T. Tysoe, Reaction of tributyl phosphite with oxidized iron: surface and tribological chemistry, *Langmuir*, 2004, **20**, 7557–7568.
- 14 A. Murase and T. Ohmori, ToF-SIMS analysis of phosphate-type lubricant additives adsorbed on friction surfaces of ferrous materials, *Surf. Interface Anal.*, 2001, **31**, 93–98.
- 15 A. W. Holbert, J. D. Batteas, A. Wong-Foy, T. S. Rufael and C. M. Friend, Passivation of Fe(110) via phosphorus deposition: the reactions of trimethylphosphite, *Surf. Sci.*, 1998, **401**, L437–L443.
- 16 A. Riga, J. Cahoon and W. R. Pistillo, Organophosphorus chemistry structure and performances relationships in FZG gear tests, *Tribol. Lett.*, 2000, **9**(3–4), 219–225.
- 17 F. T. Barcroft, A technique for investigating reactions between E.P. additives and metal surfaces at high temperature, *Wear*, 1960, **3**, 440–453.
- 18 O. Beeck, J. W. Givens and E. C. Williams, On the Mechanism of Boundary Lubrication. II, *Proc. R. Soc. London, Ser. A*, 1940, **177**(968), 103.
- 19 D. Philippon, M. I. De Barros-Bouchet, T. Le Mogne, E. Gresser and J. M. Martin, Experimental simulation of phosphites additives tribochemical reactions by gas phase lubrication, *Tribol.-Mater., Surf. Interfaces*, 2007, **1**(3), 113–123.
- 20 D. Philippon, M. I. De Barros-Bouchet, T. Le Mogne, O. Lerasle, A. Bouffet and J. M. Martin, Role of nascent metallic surfaces on the tribochemistry of phosphite lubricant additives, *Tribol. Int.*, 2011, **44**, 684–692.
- 21 D. Philippon, M. I. De Barros-Bouchet, T. Le Mogne, B. Vacher, O. Lerasle and J. M. Martin, A multi-technique approach to the characterization of iron phosphide tribofilm, *Thin Solid Films*, 2012, **524**(1), 191–196.
- 22 M. E. Merchant, Fundamentals of Cutting Fluid Action, *Lubr. Eng.*, 1950, **6**(4), 163–167.
- 23 J. A. Williams, The action of lubricants in metal cutting, *J. Mech. Eng. Sci.*, 1977, **19**(5), 202–212.
- 24 M. Boehm, J. M. Martin, C. Grossiord and T. Le Mogne, Modelling tribochemical reactions of additives by gas-phase lubrication, *Tribol. Lett.*, 2001, **11**(2), 83–90.
- 25 D. Philippon, M. I. De Barros Bouchet, T. Le-Mogne, O. Lerasle and J. M. Martin, Experimental simulation of tribochemical reactions between borates esters and steel surface, *Tribol. Lett.*, 2011, **41**(1), 73–82.
- 26 B. E. Bent, Mimicking aspects of heterogeneous catalysis: generating, isolating, and reacting proposed surface intermediates on single crystals in vacuum, *Chem. Rev.*, 1996, **4**, 1361–1390.
- 27 S. Mori and Y. Imaizumi, Adsorption of model compounds of lubricant on nascent surfaces of mild and stainless steels under dynamic conditions, *Tribol. Trans.*, 1988, **31**(4), 449–453.
- 28 H. I. Kim, J. R. Lince, O. L. Eryilmaz and A. Erdemir, Environmental effects on the friction of hydrogenated DLC films, *Tribol. Lett.*, 2006, **21**, 51–56.
- 29 M. I. De Barros Bouchet, G. Zilibotti, C. Matta, M. C. Righi, L. Vendenbulcke, B. Vacher and J. M. Martin, Lubrication of Diamond by Water Vapor and Hydrogen. Coupling Gas Phase Tribometry and Computer Works, *J. Phys. Chem. C*, 2012, **116**(12), 6966–6972.
- 30 J. P. Perdew, K. Burke and M. Ernzerhof, Generalized Gradient Approximation Made Simple, *Phys. Rev. Lett.*, 1996, **77**, 3865–3868.
- 31 P. Blonski and A. Kiejna, Structural, electronic, and magnetic properties of bcc iron surfaces, *Surf. Sci.*, 2007, **601**, 123–133.
- 32 G. Zilibotti and M. C. Righi, *Ab initio* Calculation of the Adhesion and Ideal Shear Strength of Planar Diamond Interfaces with Different Atomic Structure and Hydrogen Coverage, *Langmuir*, 2011, **27**, 6862–6867.
- 33 J. F. Moulder, W. F. Stickle, P. E. Sobol and K. D. Bomben, *Handbook of X-ray Photoelectron Spectroscopy: A Reference Book of Standard Spectra for Identification and Interpretation of XPS Data*, Perkin-Elmer, Boston, 1995.

Paper

- 34 R. G. Pearson, *Chemical Hardness*, Wiley-VCH, Weinheim, 1st edn, 1995, p. 198.
- 35 J. M. Martin, C. Grossiard, K. Varlot, B. Vacher and J. Igarashi, Tribochemical interactions between zinc dithiophosphate, molybdenum dithiocarbamate and calcium borate, *Tribol. Lett.*, 2000, **8**, 193–203.
- 36 W. Arabczyk, T. Baumann, F. Storbeck, H. J. Mussig and A. Meisel, Interaction between phosphorus and oxygen on the Fe(111) surface, *Surf. Sci.*, 1987, **189**, 190–198.
- 37 P. Blonski, A. Kiejna and J. Hanfer, Theoretical study of oxygen adsorption at the Fe(1 1 0) and (1 0 0) surfaces, *Surf. Sci.*, 2005, **590**, 88–100.
- 38 D. E. Jiang and A. E. Carter, Adsorption and dissociation of CO on Fe (110) from first principles, *Surf. Sci.*, 2004, **570**, 167–177.
- 39 G. Zilibotti, S. Corni and M. C. Righi, Load-induced confinement activates diamond lubrication by water, *Phys. Rev. Lett.*, 2013, **111**, 146101.